Modeling the gelatinization-melting transition of the starch-water system in pulses (lentil, bean and chickpea)

C. Lefèvre, P. Bohuon, L. Akissoé, L. Ollier, B. Matignon, C. Mestres

Modeling the gelatinization-melting transition of the starch-water system in pulses (lentil, bean and chickpea)

C. Lefèvre [a], P. Bohuon [a*], L. Akissoé [b], L. Ollier [a,b], B. Matignon [a,b], C. Mestres [a,b]

[a] Qualisud, Univ Montpellier, CIRAD, Institut Agro, Avignon Université, Université de La Réunion, Montpellier, France.

[b] CIRAD, UMR Qualisud, F-34398 Montpellier, France.

***Corresponding author**: Philippe Bohuon, *Institut Agro, UMR QualiSud, 1101 Av. Agropolis, 34093 Montpellier, France*. Tel: +334678740 81; Fax: +33 4 67 61 44 44. E–mail address: philippe.bohuon@supagro.fr

Keywords

Starch, Gelatinization, Melting, DSC, Modeling, Pulses

Abstract

Cooking-induced conversion of starch, the major carbohydrate in pulses, is crucial for the digestibility of the seed. The gelatinization-melting transition of lentil, bean and chickpea starches was studied using Differential Scanning Calorimetry at different temperatures (T values ranged from 20 to 160 °C) and water contents (X from 0.2 to 3 kg kg^{-1} db). Gelatinization and melting endotherms were successfully modeled as two desummed Gaussian functions. This modeling enabled to generate the degree of starch conversion for any T and X conditions, a valuable indicator that could be used in predictive cooking models. As previously reported for melting, the temperature of gelatinization was found to depend on moisture in a way that can be modeled using the Flory-Huggins equation. The results suggest that starch undergoes melting transition irrespective of water content. The similar starch conversion diagram for the three pulses suggest that starches have similar thermal behavior.

Highlights

- Overlapping gelatinization and melting peaks from DSC thermogram are desummed.
- Heat flow is successfully modeled as two Gaussian functions depending on T and X.
- Starch undergoes melting transition regardless of its water content.
- T_G, like T_M, is a function of water content modeled using the Flory-Huggins equation.
- The starch conversion diagram is similar in lentil, bean and chickpea.

41 **Abbreviations**

DSC	Differential Scanning Calorimetry
FWHM	Full Width at Half Maximum
G	First endotherm of gelatinization
M	Melting endotherm
R	Gas constant (J mol^{-1} K^{-1})
RMSE	Root-mean-square error
T	Temperature (°C)
T_i	Temperature at maximum peak i (°C)
X	Water content of starch flour (kg kg^{-1} dry basis)

Greek symbols

β_i	Dimensionless area of peak i
$\beta_{G,\infty}$	Dimensionless area of peak G in excess water
$\Delta h_{i,0}$	Change in molar enthalpy of gelatinization (i = G) or melting (i = M) per repeating unit (J mol^{-1})
ΔT_i	Parameter related to the width of peak i (°C)
$\Delta T_{i,0}$	Parameter related to the width of peak i when water content is zero (°C)
$\Delta T_{i,\infty}$	Parameter related to the width of peak i in excess water (°C)
ζ_G	Correlation parameter used to calculate β_G
v_g	Molar volume of repeating unit (m^3 mol^{-1})

v_w	Molar volume of water (m^3 mol^{-1})
τ	Degree of starch conversion
φ	Heat flow (W)
$\overline{\varphi}$	Normalized dimensionless heat flow
ϕ	Volume fraction of water in starch-water mixture (m^3 m^{-3})
χ_i	Flory interaction parameter for i transition (i = M or G)

42

43

1. Introduction

Pulses are the edible seeds from plant family *Leguminosae* (also called *Fabacae*). Hundreds of varieties are grown worldwide, especially in India (Hoover, Hughes, Chung & Liu, 2010). The FAO declared 2016 the International Year of Pulses (IYP) to promote pulses because of their potential to make food production systems more sustainable. Indeed, pulse crops provide a sustainable source of nitrogen (Crews & Peoples, 2004) which enhances soil fertility. They reduce water use and increase agricultural productivity (Gan et al., 2015). In many developing countries, pulses are already part of human and animal consumption, particularly because of their high protein content, 15-30 % db (Hoover et al., 2010). In addition, pulses contain 40-70 % db of carbohydrates, including starch (20-50 % db) and dietary fibers (15-30 % db) (Hoover et al., 2010; Tosh & Yada, 2010; Hall, Hillen & Garden Robison, 2017). Health organizations now recommend pulses in all human diets for nutritional and environmental reasons (Margier et al., 2018). However, their consumption can cause digestive problems due to the presence of anti-nutritional factors and limited knowledge about cooking procedures (Coffigniez et al., 2018a; Coffigniez et al., 2018b; Coffigniez et al., 2019). In humans, the digestive enzymes have difficulty hydrolyzing native starch, the main component of pulse seeds, because of its crystalline and granular structure. In raw pulses, the resistant starch content is high (Hoover et al., 2010). Therefore, heat treatment is required to increase the proportion of rapidly digestible starch and improve digestibility. Giraldo Toro et al. (2015) observed a strong correlation between the gelatinization rate and the digestibility of plantain starch flour. They postulated that the cooking process does not influence the final digestibility of plantain starch if the gelatinization rate is sufficient. Therefore, starch digestibility entirely depends on temperature and water content. We realized that the nutritional quality of cooked pulses could be monitored by modeling the degree of starch conversion (Briffaz, Bohuon, Méot, Dornier & Mestres, 2014). Phase diagrams of starch-water systems have already been

investigated for different food products, for example, rice (Briffaz, Mestres, Matencio, Pons & Dornier, 2013) and plantain (Giraldo Toro et al., 2015), but not pulses. Differential Scanning Calorimetry (DSC) is widely used to investigate phase transitions of starch by measuring the heat flow associated with the gelatinization and melting of starch granules when heated. The The shape of the DSC thermogram depends on the starch water content. At low water content, a biphasic endotherm is observed (Donovan, 1979). The two roughly overlapping peaks were related to the order-disorder transition and the hydration of starch crystallites, respectively (Donovan, 1979): G for gelatinization and M for melting (Donovan & Mapes, 1980). In excess water, some authors associated the single apparent peak with the G endotherm (Donovan, 1979), while others consider that the DSC signal could hide a small peak M, which overlaps the dominant peak G (Blanshard, 1987; Tananuwong & Reid, 2004), suggesting that starch undergoes both order-disorder transition and melting in excess water. The aim of this study was to investigate gelatinization and melting transitions of starch-water system using DSC to model a starch conversion diagram specific to pulses. This tool could be applied to develop a predictive cooking model to improve the nutritional value of pulses. We used a desummation procedure in an attempt to dissociate the gelatinization and melting events. Three pulse varieties (lentil, bean and chickpea) were analyzed to compare the thermal behavior of pulses with different physiochemical and morphological characteristics. These three varieties are the most commonly eaten in France (Margier et al., 2018).

2. Materials and methods

2.1 Material

Green lentils (*L. culinaris,* var. Anicia), navy beans (*P. vulgaris*, var. Linex) and chickpeas (*C. arietinum*, var. Elvar) were provided by Cibèle (Saint-Georges-Sur-Arnon, France), Cavac (La Roche-sur-Yon, France) and Moulin Marion (Saint-Jean-sur-Veyle, France), respectively.

The lentils were harvested in 2017 and the beans and chickpeas in 2018. All seeds were stored in a vacuum pack at 7 °C until use.

2.2 Starch extraction

Starch was first extracted from the pulses using dry fractionation. The lentil hulls were removed from the seeds with dry abrasion using a DMS 500 huller (Electra, Poudenas, France). Dehulled lentils were sieved through a 2 mm mesh screen to separate the hull residues. Dry fractionation of chickpeas and beans was performed by Improve SAS (Dury, France). The seeds were crushed at 700 rpm using a SM 300 cutting mill (Retsch GmbH, Haan, Germany), equipped with a 8 mm sieve. The hulls were removed from the kernels using a MZM 1-40 zigzag air classifier (Hosokawa Micron, Evry, France). The dehulled pulses were ground into flour at different speeds (18 000 rpm for lentils and 20 000 rpm for beans and chickpeas), using a high speed impact mill UPZ equipped with a pill mill (Hosokawa Alpine, Augsburg, Germany). Starch and protein fractions from the resulting flours were separated using an ATP air classifier (Hosokawa Alpine, Augsburg, Germany) at 6 500 rpm for lentils, 8 000 rpm for beans and 10 000 rpm for chickpeas. The coarse fraction from lentils was ground and air classified once again to improve the fine fraction yield, according to Tyler, Youngs & Sosulki (1981). The resulting coarse fractions from all pulses were rich in starch but additional starch purification was performed using wet separation. Coarse fractions were suspended in water and centrifuged at 5 000 rpm. The pellet was recovered, wet purified a second time and then dried at 45°C. All starch samples were stored at 14 °C.

2.3 Water and total starch content

Water content of the starch sample was calculated on a wet basis by drying 5 g of each pulse starch sample for 2 h at 132 °C (± 2 °C) according to the standard method NF EN ISO 712

(2010). Total starch content was estimated using the enzymatic procedure according to Holm, Björck, Drews & Asp (1986).

2.4 Differential scanning calorimetry

Thermal transitions associated with starch gelatinization and melting were determined using a DSC 8500 instrument (Perkin Elmer, Norwalk, USA) calibrated with indium as standard. Starch flour was weighed in stainless steel pans and deionized water was added using a micropipette. The amount of water was adjusted to obtain a water content X ranging from 0.2 to 3 kg kg^{-1} db (kg water/kg dry starch), to study starch samples from low to excess moisture conditions. The total weight of each sample was approximately 40 mg. The pans were hermetically sealed and allowed to stabilize at 14 °C between 5h and 24h before analysis, depending on the water content of the sample. The pans were then heated from 20 °C to 160 °C at a rate of 10 °C/min, with an empty sealed pan as reference. First, 14 different water contents were performed for lentil, as presented in Table 1. Since some resulting heat flows were similar, the number of moisture conditions has been reduced to 10 and 13 for bean and chickpea, respectively. For lentil and chickpea, at $X = 0.2$ kg kg^{-1} db the temperature at the end of starch conversion exceeded 160 °C. To prevent damage to the pan due to the increasing pressure inside, the maximum temperature of heating could not exceed 160°C under the experimental conditions of the study. Therefore, the corresponding DSC thermograms were not analyzed. All measurements were duplicated. In total, 28, 20 and 26 samples were measured for lentil, bean and chickpea flour, respectively. A blank thermogram (empty pans in reference and sample ovens) was recorded daily. The heat flow (mW) of sample pans minus the variation of heat flow of the blank during heating was recorded using the Pyris Thermal Analysis Software (Perkin Elmer, Norwalk, USA).

Table 1. Experimental conditions of the database by pulse type: water content (X) of starch samples analyzed with DSC from 20 °C to 160 °C.

X (kg kg^{-1} db)	Lentil	Bean	Chickpea
0.2	nd	×	nd
0.3	×	–	×
0.4	×	×	×
0.5	×	×	×
0.6	×	×	×
0.8	×	×	×
1.0	×	×	×
1.2	×	–	–
1.5	×	×	×
1.6	×	–	×
1.8	×	×	×
2.0	×	×	×
2.5	×	–	×
3.0	×	×	×

×: measured in duplicate

nd: incomplete signal detected by DSC at $T \leq 160$ °C

–: not tested

2.5 Starch conversion diagram modeling

DSC thermograms plot heat flow (ϕ) as a function of temperature (T). In excess water, a single endotherm is observed at low temperature and commonly assigned to the gelatinization process (G) (Donovan, 1979). With decreasing water content, a second endotherm appears at higher temperature. It was described as the melting (M) of starch granules (Donovan, 1979). The two roughly overlapping peaks were desummed as a function of T and X. The degree of starch conversion was calculated using the model and represented as a diagram.

2.5.1 Modeling the DSC peaks

DSC thermogram data (ϕ versus T) were analyzed using a desummation procedure with two Gaussian functions illustrated in Fig. 1. First, a baseline was subtracted from the heat flow to

157 simplify the process of curve fitting. The resulting heat flow was non-dimensionalized and
158 multiplied by 1000, to avoid low parameter values by increasing the scale. Lastly, each
159 dimensionless value for heat flow ($\overline{\varphi}$) was fitted in relation to the sum of two peaks (i = G or
160 M) as follows:

161 $$\overline{\varphi} = \sum_{i=\mathrm{G,M}} \frac{\beta_i}{\Delta T_i \sqrt{2\pi}} \exp\left(-\frac{1}{2}\left(\frac{T - T_i}{\Delta T_i} \right)^2 \right) \quad (1)$$

162 where T_i (°C) is the temperature at maximum peak i; ΔT_i (°C) controls the width of the peak i
163 and is related to the full width at half maximum (FWHM) of the peak i according to
164 $2\sqrt{2\ln(2)} \times \Delta T_i = \mathrm{FWHM}$; β_i is the dimensionless area of peak i. Therefore:

165 $$\int_{-\infty}^{\infty} \overline{\varphi} = \beta_G + \beta_M = 1 \quad (2)$$

166 Parameters from Eq. (1) depend on the water content X in the starch-water mixture.

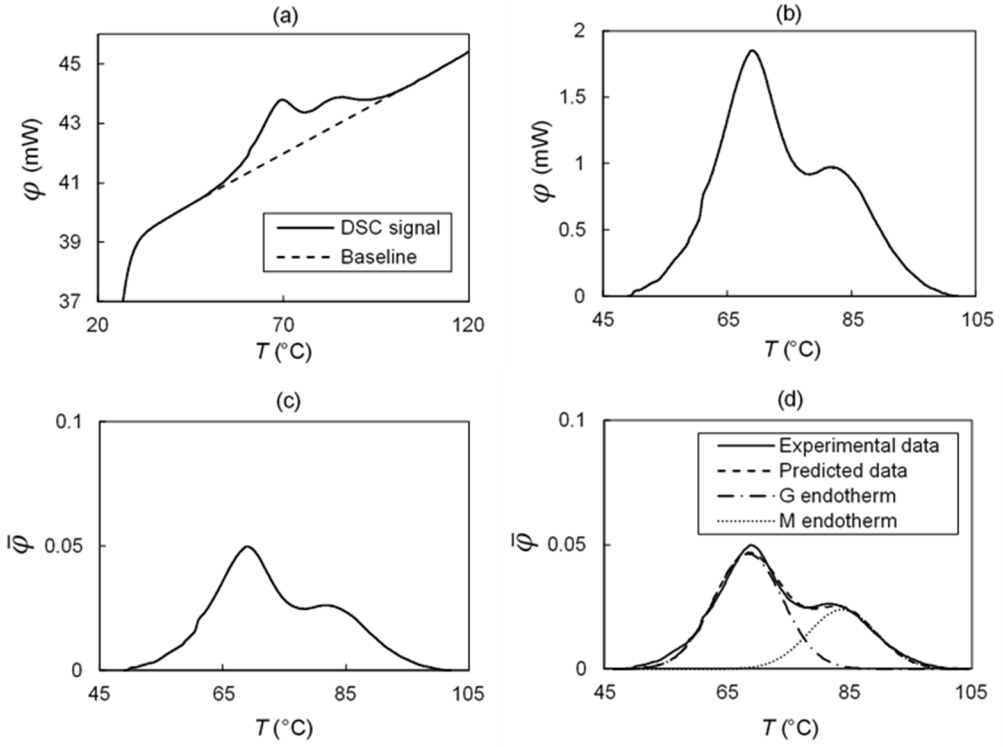

167

168 Figure 1. Graphical explanation of the desummation procedure: (a) a baseline (--) was defined
169 for each DSC thermogram (solid line); (b) heat flow obtained after subtraction of the baseline;

(c) heat flow obtained after non-dimensionalization and multiplication by 1000; (d) the dimensionless heat flow (solid line) was modeled as a bi-Gaussan function (--) showing desummed G (-.-) and M (···) endotherms.

2.5.2 *Peak temperatures*

The Flory–Huggins equation (Flory, 1953) was used to describe the relation between T_i (i = G or M) and the volume fraction of the water (ϕ) in the starch-water mixture:

$$\frac{1}{T_i} - \frac{1}{T_{i,0}} = \frac{R}{\Delta h_{i,0}} \frac{v_g}{v_w} \left(\phi - \chi_i \, \phi^2 \right) \tag{3}$$

Where $\Delta h_{i,0}$ (J mol^{-1}) is the change in the molar enthalpy of gelatinization (i = G) or melting (i = M) per repeating unit (anhydroglucose); v_g / v_w is the ratio of the molar volume of the repeating unit ($v_g = 105.0 \times 10^{-6}\,\mathrm{m^3 mol^{-1}}$) to the molar volume of the water ($v_w = 18.1 \times 10^{-6}\,\mathrm{m^3 mol^{-1}}$) and, therefore, $v_g / v_w = 5.8$; R is the gas constant (8.31 J mol^{-1} K^{-1}); $T_{i,0}$ (K) is the gelatinization (i = G) or melting (i = M) temperature of the pure polymer and χ_i is the Flory interaction parameter. To calculate ϕ, the density of water was taken to be 1 000 kg m^{-3} and the density of starch was attributed an average value of 1 500 kg m^{-3} (Cruz-Orea et al., 2002). Therefore, ϕ (m^3 m^{-3}) was expressed as a function of water content X:

$$\frac{1}{\phi} = 1 + \frac{1}{1.5X} \tag{4}$$

2.5.3 *Peak widths*

188 The width-related parameter ΔT_i represents the fact that, within one sample at fixed water
189 content, starch granules have slightly various sizes and compositions. This leads to individual
190 variations in the gelatinization or melting temperature and so broad peaks on DSC
191 thermogram (Carlstedt, Wojtasz, Fyhr & Kocherbitov, 2015). ΔT_i decreases as a function of
192 water content. An empirical relation was used to describe ΔT_i as a function of *X*:

193 $$\frac{\Delta T_i - \Delta T_{i,\infty}}{\Delta T_{i,0} - \Delta T_{i,\infty}} = \exp\left(-\frac{X}{\gamma_i}\right) \quad (5)$$

194 where $\Delta T_{i,0}$ (°C) and $\Delta T_{i,\infty}$ (°C) are the values for ΔT_i, with zero and excess water contents,
195 respectively; γ_i is the rate parameter of decrease for the two correlations. For melting, γ_M
196 was not significantly different from 1. Its value was thus fixed at 1 to simplify the expression
197 of ΔT_M with only 2 water-dependent variables.

198 *2.5.4 Amplitude of the peak area*

199 With increasing water content, β_G increases and β_M decreases as shown by Eq. (2). A simple
200 empirical equation was used to describe β_i as a function of *X*:

201 $$\beta_G = \beta_{G,\infty}\exp\left(-\frac{\zeta_G}{X}\right) \quad (6a)$$

202 where $\beta_{G,\infty}$ is the dimensionless area of peak G in excess water and ζ_G is a parameter for the
203 correlations. β_M was calculated with Eq. (2) and (6a):

204 $$\beta_M = 1 - \beta_{G,\infty}\exp\left(-\frac{\zeta_G}{X}\right) \quad (6b)$$

205 *2.5.5 Degree of starch conversion*

206 The degree of starch conversion τ was defined for any temperature *T* and water content *X* as
207 the ratio between the enthalpy change calculated from the beginning of peak G to *T*, and the
208 whole enthalpy change from the beginning of peak G to the end of peak M (Eq. (7a)). The
209 integral of the sum of Gaussian functions is the sum of error functions (Eq. (7b)).

210 $$\tau = \int_0^T \overline{\varphi}(T,X) \Big/ \int_0^\infty \overline{\varphi}(T,X) \quad (7a)$$

211 $$\tau = \sum_{i=\mathrm{G,M}} \beta_i \times \frac{1}{2}\left(1+\mathrm{erf}\left(\frac{T-T_i}{\Delta T_i\sqrt{2}}\right)\right) \quad (7b)$$

212 Finally, isovalues lines of degree of starch conversion τ were represented as a temperature *T*
213 versus water content *X* diagram.

214 *2.5.6 Parameters identification for modeling the starch conversion diagram*

215 Two different procedures, referred to as sequential and overall identification methods, were
216 used and compared to identify the parameters. The sequential procedure consisted of two
217 steps. The first step involved identifying the 6 so-called primary parameters (T_i, ΔT_i and β_i)
218 in the DSC peak desummation model, by fitting dimensionless heat flow thermograms to
219 Eq. (1) for each water content *X*. The second step involved identifying the 13 so-called
220 secondary parameters ($T_{i,0}$, Δh_i, χ_i, $\Delta T_{i,\infty}$, $\Delta T_{i,0}$, γ_G, $\beta_{\mathrm{G},\infty}$ and ζ_G) used to described the
221 primary parameters as functions of *X*. They were identified by fitting primary parameters to
222 Eq. (3), (5) and (6a), respectively. The aim of the overall procedure was to identify the 13
223 secondary parameters at the same fitting session, by fitting all dimensionless heat flow
224 thermograms to the model combining Eq. (3), (5) and (6a) within Eq. (1). The curve fitting
225 toolbox (Matlab software, version R2019b, The MathWorks Inc., Natick, USA) with the
226 Levenberg-Marquardt algorithm was used to identify all parameters.

2.6 *Statistical methods*

The parameter values obtained from the two identification methods are given with a 95 % confidence level. The root-mean-square error (RMSE) was calculated between the dimensionless heat flow DSC thermograms (experimental data) and the dimensionless heat flows predicted by sequential and overall identification methods.

3. Results and Discussion

3.1 *Starch characterization*

The total starch content of starch flour was estimated at 95.2 % (*i.e.* kg starch/kg flour on a dry basis) for lentils, 96.8 % for beans and 92.1 % for chickpeas. Therefore, the thermal behavior of all starch flours was considered to be close to that of a pure starch-water mixture. The water content of starch flour was 12.2 % (*i.e*. kg water/kg flour) for lentils, 11.5 % for beans and 11.1 % for chickpeas.

3.2 *Modeling the starch conversion diagram*

3.2.1 *Modeling the DSC peaks*

The experimental DSC thermograms show that the thermal behavior of the starch-water system is similar for the three pulses. The primary parameters identified using the desummation procedure (Eq. (1)) are presented in Fig. 2 with dots. At water contents below 2 kg kg^{-1} db, the presence of a biphasic endotherm meant it was easy to identify the so-called G and M peaks (Donovan & Mapes, 1980) and, therefore, the primary parameters. With increasing water content, the DSC signal has a single peak (which may be followed by a small shoulder that decreases in size), as reported for cereals, plantain and peas in the literature (Donovan, 1979; Cruz-Orea, Pitsi, Jamée & Thoen, 2002; Tananuwong & Reid, 2004; Briffaz

et al., 2013; Giraldo Toro et al., 2015). According to Eq. (1), there are two possible mathematical interpretations for this shape. The first assumes that T_M is higher than T_G and β_G is close to 1. The second assumes that T_M and T_G are close and that β_G and β_M are also close. According to the second hypothesis, the melting transition makes a greater contribution to starch conversion than suggested in the first hypothesis. As the RMSE of the two non-linear regressions were closed (data not shown), we chose the first hypothesis to identify the primary parameters. Indeed, we do not yet fully understand the thermal transitions that appear on the DSC thermogram. Many theories proposed in the literature describe starch changes during gelatinization and melting. Donovan (1979) first suggested that swelling in the amorphous region of starch granules in the presence of water causes the disruption of crystalline parts by "stripping" starch chains on the surface. If there is sufficient water, all starch crystallites can be moisturized and melt cooperatively, resulting in a single peak on the heat flow thermogram. If water is limited, the remaining low-hydrated crystallites melt at a higher temperature, resulting in a biphasic endotherm. Evans & Haisman (1982) proposed that the two peaks were due to the different crystallite stability. The granules with less stable crystallites melt, which produces the first peak. This reduces the available water and, as a result, the more stable crystallites that remain melt at a higher temperature. With increasing water, the melting temperature decreases and, thus, the second peak shifts towards the first. Numerous other theories have been proposed and were reported by Ratnayake & Jackson (2007). In their study, they described starch gelatinization as a complex process that cannot be reduced to order-disorder transition because it induces structural and morphological changes in starch granules. They reported greater mobility of starch polymers and amylose molecules due to water absorption in the amorphous regions. This mobility leads to the formation of new intermolecular bonds, which occurs simultaneously to the so-called gelatinization process. They also highlighted that DSC measurements were unable to provide this type of information

with regard to polymer structure at low temperature. In the present study, starch was thus supposed to undergo gelatinization and melting according to one of the previous hypothesis. Since the aim of the study was modeling the degree of starch conversion, we did not perform further analysis of the starch morphology. To validate which hypothesis best describes the starch conversion under the conditions of the study, complementary techniques should be carry out, such as microscopy (Ratnayake & Jackson, 2007). For example, by combining the results from optical microscopy, X-ray scattering and DSC up to 100 °C, Carlstedt et al. (2015) showed that G and M endotherms could be interpreted as a eutectic transition and a liquidus line, respectively.

3.2.2 *Parameters identification from the sequential method*

The identification of primary parameters shows that the temperature of gelatinization (Fig. 2a) and melting (Fig. 2b), the width (Fig. 2c and 2d) and the relative area (Fig. 2e) of each peak depend on the starch water content. This phenomenon has been observed by many authors (Donovan, 1979; Evans & Haisman, 1982; Cruz-Orea et al., 2002; Tananuwong & Reid, 2004; Briffaz et al., 2013). These trends are modeled with the 13 secondary parameters obtained from the sequential identification method and presented in Table 2.

For all studied pulses, the Flory-Huggins equation provides a satisfactory description of the relation between T_{M} and ϕ (Fig. 2b). Overall, the corresponding secondary parameters obtained using the sequential identification method (Table 2) are in the same order as those found in previous studies. We found $T_{\mathrm{M},0}$ values ranging from 227.6 ± 25.0 °C to 307.8 ± 37.5 °C, $\Delta h_{\mathrm{M},0}$ values from 16.4 ± 8.7 kJ mol^{-1} to 23.8 ± 4.4 kJ mol^{-1} and χ_{M} values from 0.62 ± 0.05 to 0.65 ± 0.3 depending on pulse species. Previous studies, focusing mainly on cereals and potato starches, reported $T_{\mathrm{M},0}$ values ranging from 167 °C to 258 °C, $\Delta h_{\mathrm{M},0}$

298 values from 12.6 kJ mol^{-1} to 54.4 kJ mol^{-1} and χ_M values from 0.48 to 0.51 (Donovan,
299 1979; Donovan & Mapes, 1980; Farhat & Blanshard, 1997; Cruz-Orea et al., 2002; Habeych,
300 Guo van Soest, van der Goot & Boom, 2009; van der Sman & Meinders, 2011).
301 Donovan (1979) reported that the maximum for the G endotherm was always observed at
302 66 °C for potato starches with ϕ ranging from 0.28 to 0.81. Our results show that T_G can
303 indeed be considered constant around 66 °C when the water content is sufficient (*i.e.*
304 $X > 0.7$ kg kg^{-1} db; $\phi > 0.5$ m^3 m^{-3}). An isothermal temperature of gelatinization has also
305 been reported by Carlstedt et al. (2015) for the same range of water content. However, T_G
306 increases at a lower water content for all pulses (Fig. 2a). This observation is consistent with
307 the results presented by Evans & Haisman (1982). They reported a constant initial
308 temperature of gelatinization for water content above 0.6 kg kg^{-1} db and a steep increase in
309 temperature with a decreasing water content. Thus, given the range of water contents under
310 study, T_G can be plotted as a function of ϕ according to the Flory-Huggins equation with a
311 good fitting result (Fig. 2a). The secondary parameters obtained using the sequential
312 identification method (Table 2) differ from those previously reported for peak M. $T_{G,0}$ is
313 lower than $T_{M,0}$ and $\Delta h_{G,0}$ is higher than $\Delta h_{M,0}$.
314 The width of G and M endotherms (ΔT_G and ΔT_M) decreases with water content (Fig. 2c and
315 1d), as reported in previous studies (Donovan, 1979; Tananuwong & Reid, 2004). The β_G
316 value shows that gelatinization becomes the predominant thermic event (*i.e.* $\beta_G \geq 0.5$) when
317 the water content exceeds 1 kg kg^{-1} db for all pulses (Fig. 2e). Blanshard (1987) suggested
318 that G and M endotherms merged at high water content, resulting in a single apparent peak.
319 Tananuwong & Reid (2004) confirmed this hypothesis using instrumental and mathematical

deconvolution procedures. Sequentially-determined $\beta_{G,\infty}$ is associated with a high confidence interval (Table 2). Therefore, the melting in excess water (*i.e.* $\beta_{G,\infty} < 1$) cannot be confirmed here by simply considering the results of the sequential method. However, the trailing shoulder after the peak G at $X = 2$ kg kg^{-1} db for all pulses seems to support this hypothesis. The same also applies to some extent at $X = 3$ kg kg^{-1} db for lentil and bean. This can be seen in Fig. 3a, 4a and 5a, which represent predicted dimensionless heat flows calculated with sequentially-determined secondary parameters in comparison with experimental dimensionless heat flows for lentil, bean and chickpea, respectively. The RMSE between experimental and predicted dimensionless heat flows were calculated for each sample tested (Fig. 3a, 4a and 5a).

3.2.3 *Parameter identification from overall method*

The 13 secondary parameters obtained using the overall identification method are presented in Table 2. Confidence intervals at 95 % are lower than those from the sequential method (Table 2), which leads to more precise modeling. The predicted dimensionless heat flows calculated with the secondary parameters obtained using the overall identification method are plotted in Fig. 3b, 4b and 5b with the associated RMSE between experimental and predicted dimensionless heat flows. These results are quite close to the predicted heat flows obtained using the sequential method (Fig. 3a, 4a and 5a) for lower water content ($X < 2$ kg kg^{-1} db), with similar RMSE. The significant difference between the two methods is the position and contribution of peak M for water contents above 2 kg kg^{-1} db. This is clearly shown by the value of $\beta_{G,\infty}$, which is significantly lower than that identified using the sequential method (Table 2) for all pulses. We found $\beta_{G,\infty} = 0.61 \pm 0.01$ for lentil, 0.49 ± 0.01 for bean and 0.66 ± 0.02 for chickpea with the overall identification method. This indicates that melting is

343 important for starch conversion in excess water, even if the DSC signal has a single peak. Our
344 results are similar to the desummation curves presented by Tananuwong & Reid (2004) for
345 potato, pea and normal and waxy corn starches, who postulated that the M endotherm is
346 gradually incorporated into the predominant G endotherm. Their study shows a relative peak
347 area of G and M endotherms which is also very similar to Fig. 2e. The desummation results
348 obtained from the overall identification method confirms that G and M endotherms can be
349 merged in one peak in excess water conditions.
350
351 For chickpea and bean, when all the water contents analyzed are considered together, the
352 predictions for the dimensionless heat flows are slightly more precise with the overall method
353 (0.34% and 0.45% errors on predicted values, respectively) compared to the sequential
354 method (0.50% and 0.52% errors on predicted values, respectively). For lentil, the two
355 methods are equally precise (0.28%), as expected when comparing Fig. 3a and 3b.
356

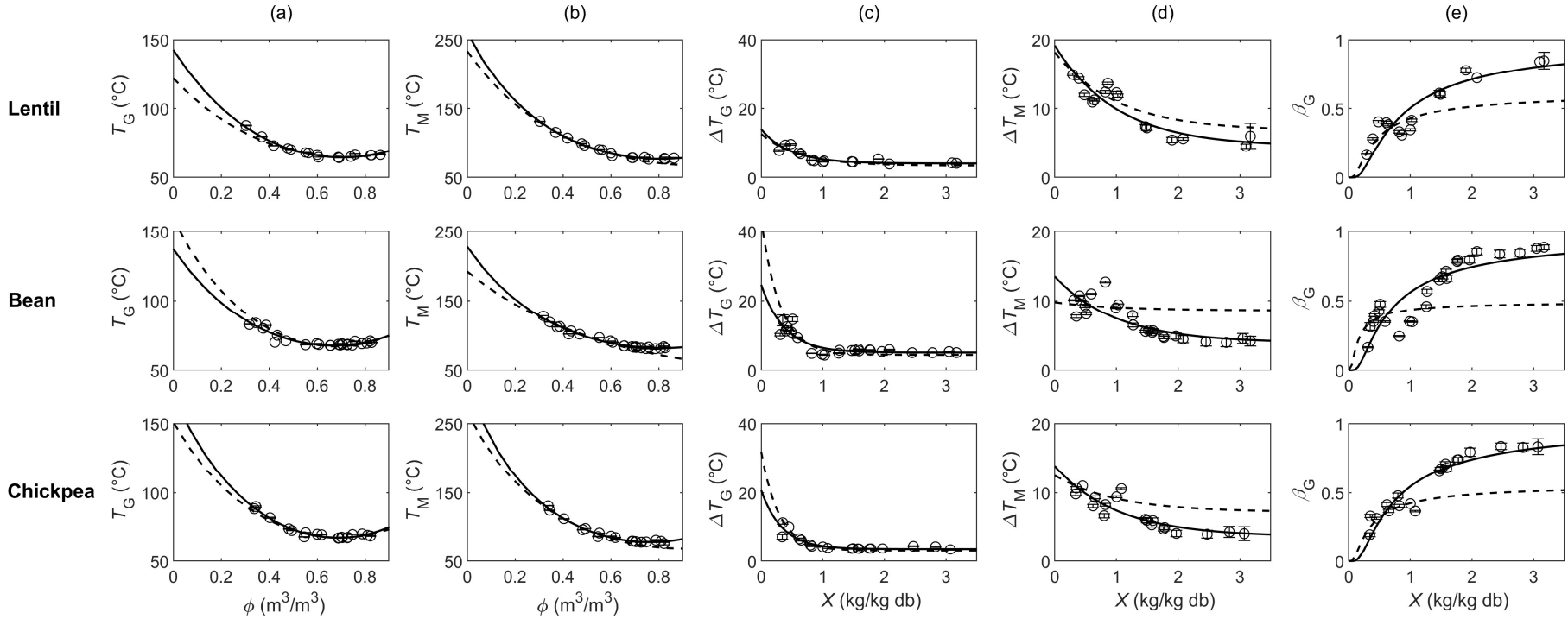

Figure 2. Primary parameters of the Gaussian functions modeled as a function of volume fraction of water ϕ or as a function of water content X for lentil, bean and chickpea starches. Primary parameters (dots) were obtained using the desummation procedure and fitted to Eq. (3) (a,b), Eq. (5) (c,d) and Eq. (6a) (e), respectively (solid lines). Results from the overall identification method (--) were later added for comparison, but were not fitted directly from the primary parameters.

363 Table 2. Secondary parameters obtained using the sequential (S) and overall (O) identification method for lentil, bean and chickpea starches

Type of starch	$\frac{1}{T_i}-\frac{1}{T_{i,0}}=\frac{R}{\Delta h_{i,0}}\frac{v_g}{v_w}\left(\phi-\chi_i\,\phi^2\right)$	$\frac{\Delta T_i-\Delta T_{i,\infty}}{\Delta T_{i,0}-\Delta T_{i,\infty}}=\exp\left(-\frac{X}{\gamma_i}\right)$	$\beta_{\mathrm{G}}=\beta_{\mathrm{G},\infty}\exp\left(-\frac{\zeta_{\mathrm{G}}}{X}\right)$

364 (mean values ± 95 % confidence interval). The values were used to calculate the degree of starch conversion $\tau=\sum_{i=\mathrm{G,\,M}}\beta_i\times\frac{1}{2}\left(1+\mathrm{erf}\left(\frac{T-T_i}{\Delta T_i\sqrt{2}}\right)\right)$

		$T_{G,0}$ (°C)	$T_{M,0}$ (°C)	$\Delta h_{G,0}$ (kJ mol^{-1})	$\Delta h_{M,0}$ (kJ mol^{-1})	χ_G	χ_M	$\Delta T_{G,0}$ (°C)	$\Delta T_{M,0}$ (°C)	$\Delta T_{G,\infty}$ (°C)	$\Delta T_{M,\infty}$ (°C)	γ_G	$\beta_{G,\infty}$	ζ_G
Lentil	S	142.5 ±9.6	260.1 ±19.5	30.5 ±3.8	19.8 ±2.0	0.71 ±0.02	0.62 ±0.03	13.99 ±6.17	19.14 ±2.42	3.99 ±0.97	4.51 ±1.45	0.47 ±0.33	1.00 ±0.16	0.69 ±0.21
	O	121.6 ±1.6	233.1 ±2.5	40.9 ±1.0	24.3 ±0.4	0.69 ±0.01	0.52 ±0.01	12.64 ±0.78	18.15 ±0.37	3.37 ±0.05	6.79 ±0.13	0.61 ±0.04	0.61 ±0.01	0.36 ±0.02
Bean	S	137.1 ±17.1	227.6 ±25.0	32.4 ±8.1	23.8 ±4.4	0.75 ±0.04	0.62 ±0.05	24.61 ±14.24	13.49 ±1.95	5.03 ±1.14	3.92 ±1.11	0.38 ±0.27	0.98 ±0.14	0.56 ±0.19
	O	158.5 ±4.3	192.1 ±1.8	26.3 ±0.9	36.8 ±0.9	0.74 ±0.01	0.36 ±0.01	43.21 ±4.49	9.79 ±0.28	4.37 ±0.06	8.62 ±0.12	0.31 ±0.01	0.49 ±0.01	0.13 ±0.02
Chickpea	S	170 ±14.4	307.8 ±37.2	24.3 ±3.3	16.4 ±8.7	0.73 ±0.02	0.65 ±0.03	20.64 ±11.53	13.89 ±1.92	3.63 ±0.77	3.63 ±1.06	0.34 ±0.20	1.01 ±0.12	0.61 ±0.16
	O	150.9 ±3.3	265.4 ±3.0	28.9 ±0.9	20.4 ±0.4	0.72 ±0.01	0.55 ±0.01	31.88 ±4.79	12.50 ±0.38	3.21 ±0.05	7.18 ±0.16	0.29 ±0.02	0.56 ±0.02	0.28 ±0.02

ϕ : volume fraction of water (m^3 m^{-3})

X : water content (kg kg^{-1} db)

γ_M is fixed at 1.

$\beta_M = 1 - \beta_G$

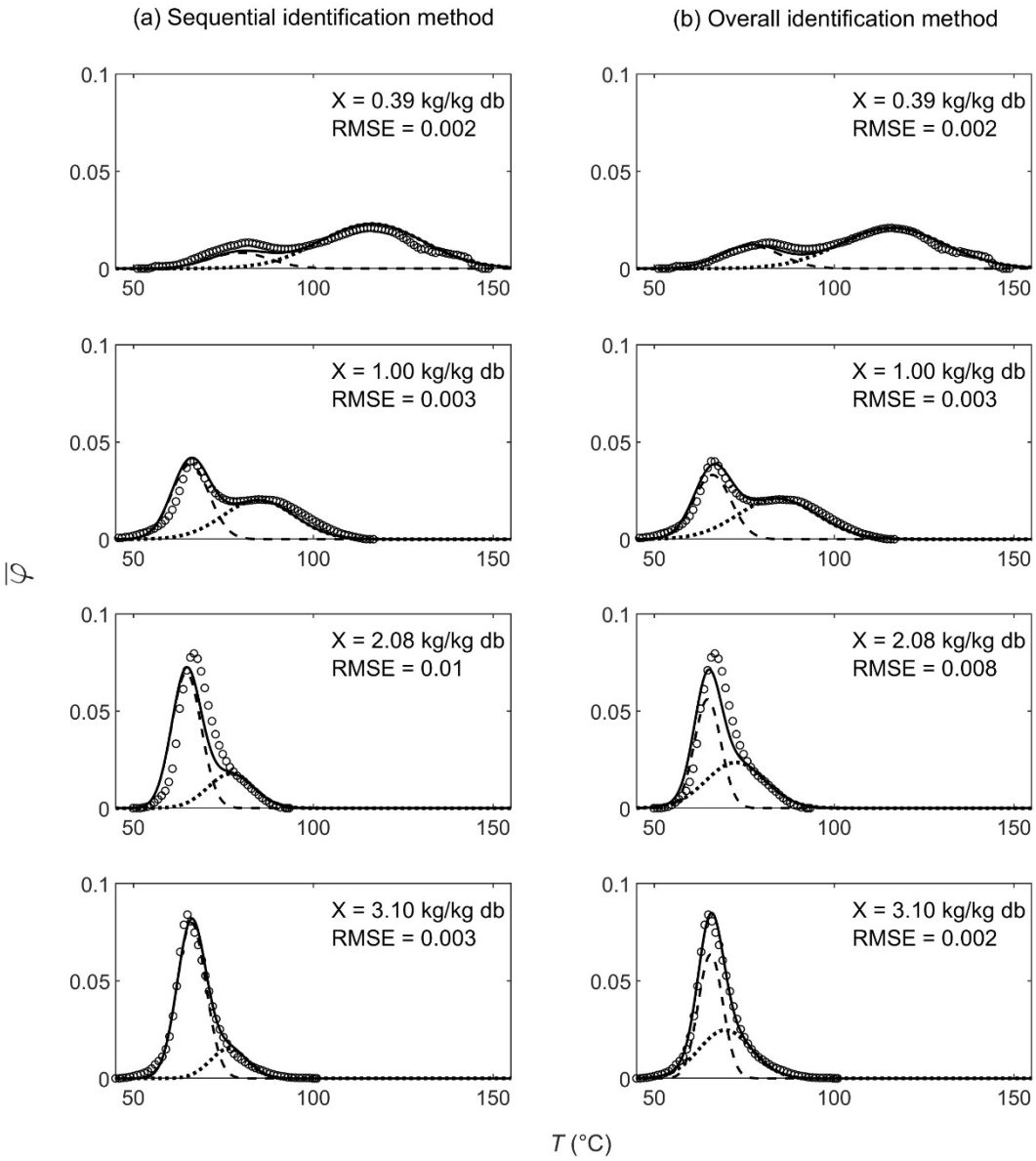

370
371 Figure 3. DSC thermograms of lentil starch at different water contents *X*: experimental (dots)
372 and predicted (solid lines) dimensionless heat flows, predicted G (--) and M (···) endotherms.
373 Predicted data were obtained using the sequential (a) and overall (b) identification method.
374 RMSE were calculated between experimental and predicted dimensionless heat flows for the
375 different water contents.
376

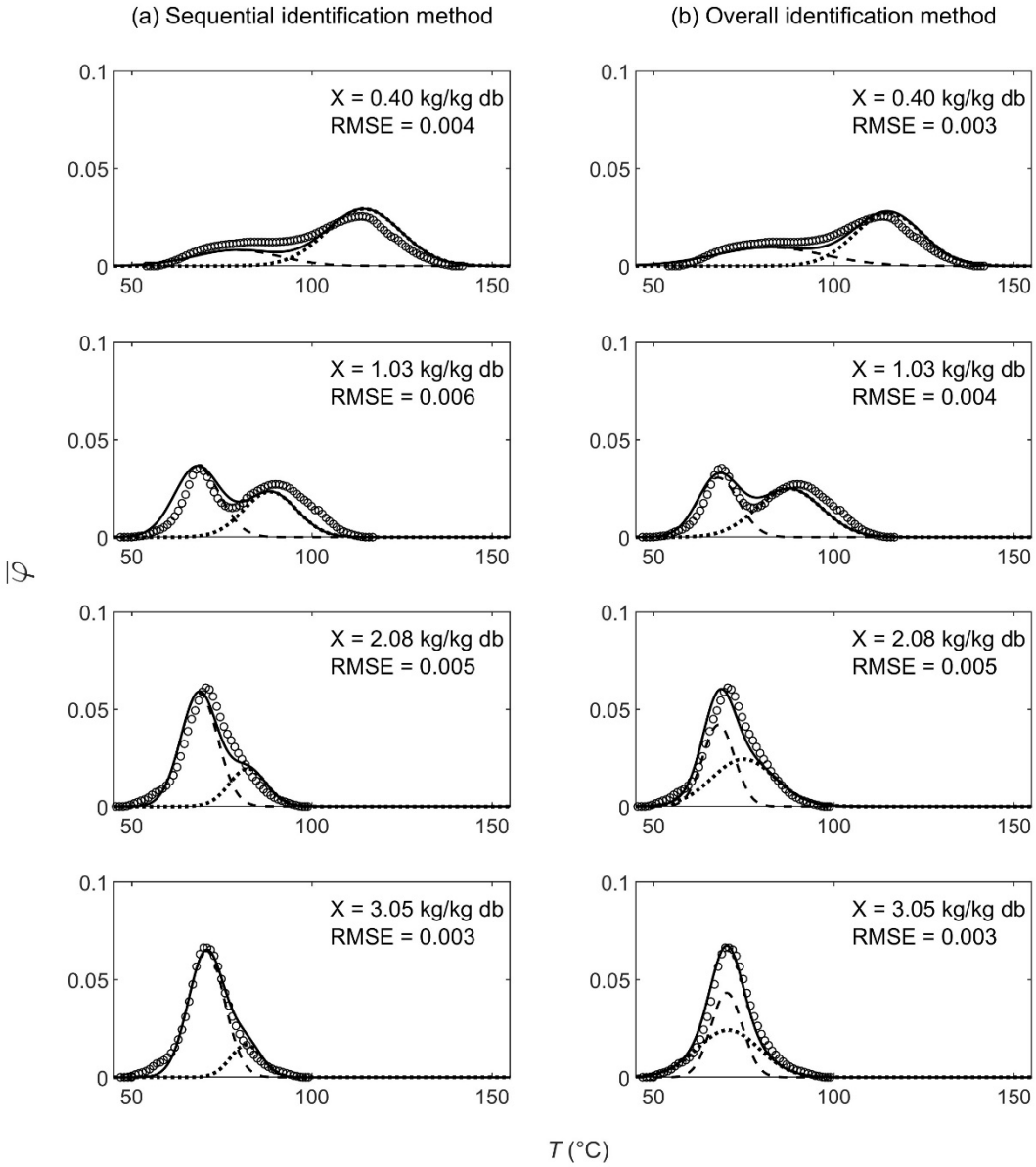

377
378 Figure 4. DSC thermograms of bean starch at different water contents *X*: experimental (dots)
379 and predicted (solid lines) dimensionless heat flows, predicted G (--) and M (···) endotherms.
380 Predicted data were obtained using the sequential (a) and overall (b) identification method.
381 RMSE were calculated between experimental and predicted dimensionless heat flows for the
382 different water contents.

383

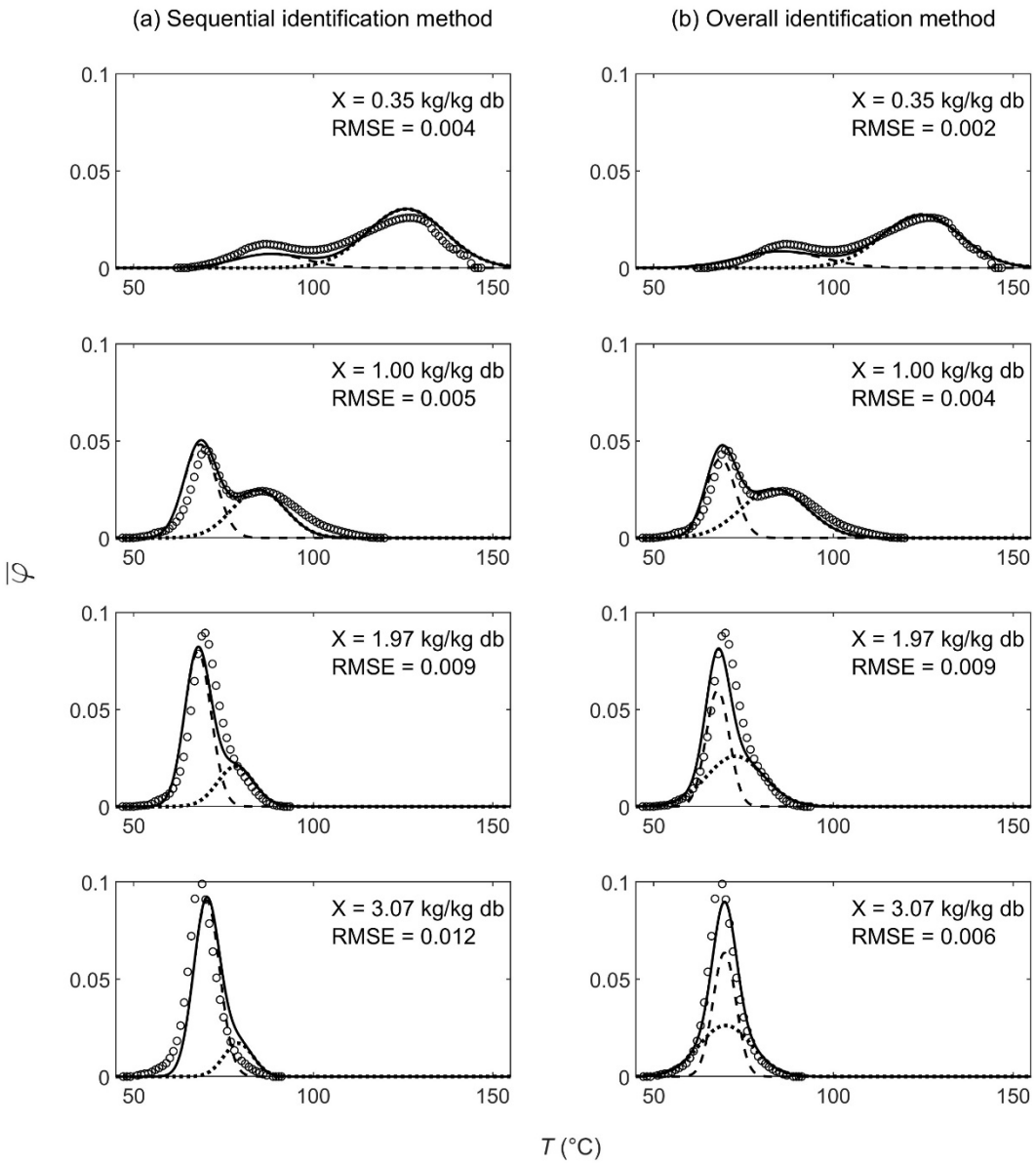

384

385 Figure 5. DSC thermograms of chickpea starch at different water contents *X*: experimental
386 (dots) and predicted (solid lines) dimensionless heat flows, predicted G (--) and M (···)
387 endotherms. Predicted data were obtained using the sequential (a) and overall (b)
388 identification method. RMSE were calculated between experimental and predicted
389 dimensionless heat flows for the different water contents.

390

3.2.4 Starch conversion diagram

For lentil, the modeled diagrams of starch conversion obtained using the sequential and overall identification methods are similar (Fig. 6a). This is consistent with the similar results obtained from both methods, as discussed previously. For bean and chickpea (Fig. 6b and 6c), the two identification methods lead to different starch conversion diagrams when τ approaches 0. With the sequential method, the temperature at the beginning of gelatinization (*line 1* in Fig. 6) increases with water content when $X > 1.5$ kg kg^{-1}. The overall method seems to reduce side effects in excess water, by giving a constant temperature at the beginning of gelatinization when $X > 1.5$ kg kg^{-1}. For the three pulses, the starch conversion diagram obtained using the overall identification method thus appears to be more accurate. Moreover, isovalue lines of starch conversion degree defined three areas (native, partially gelatinized and fully gelatinized starch) which are consistent with the scanning electron microscopy images presented by Ratnayake & Jackson (2007) on various cereal and tuber starches.

Lentil, bean and chickpea have similar starch conversion diagrams as shown in Fig. 7, suggesting that starches have similar thermal behavior. Further analysis could be performed with other varieties in order to confirm this trend in all pulses.

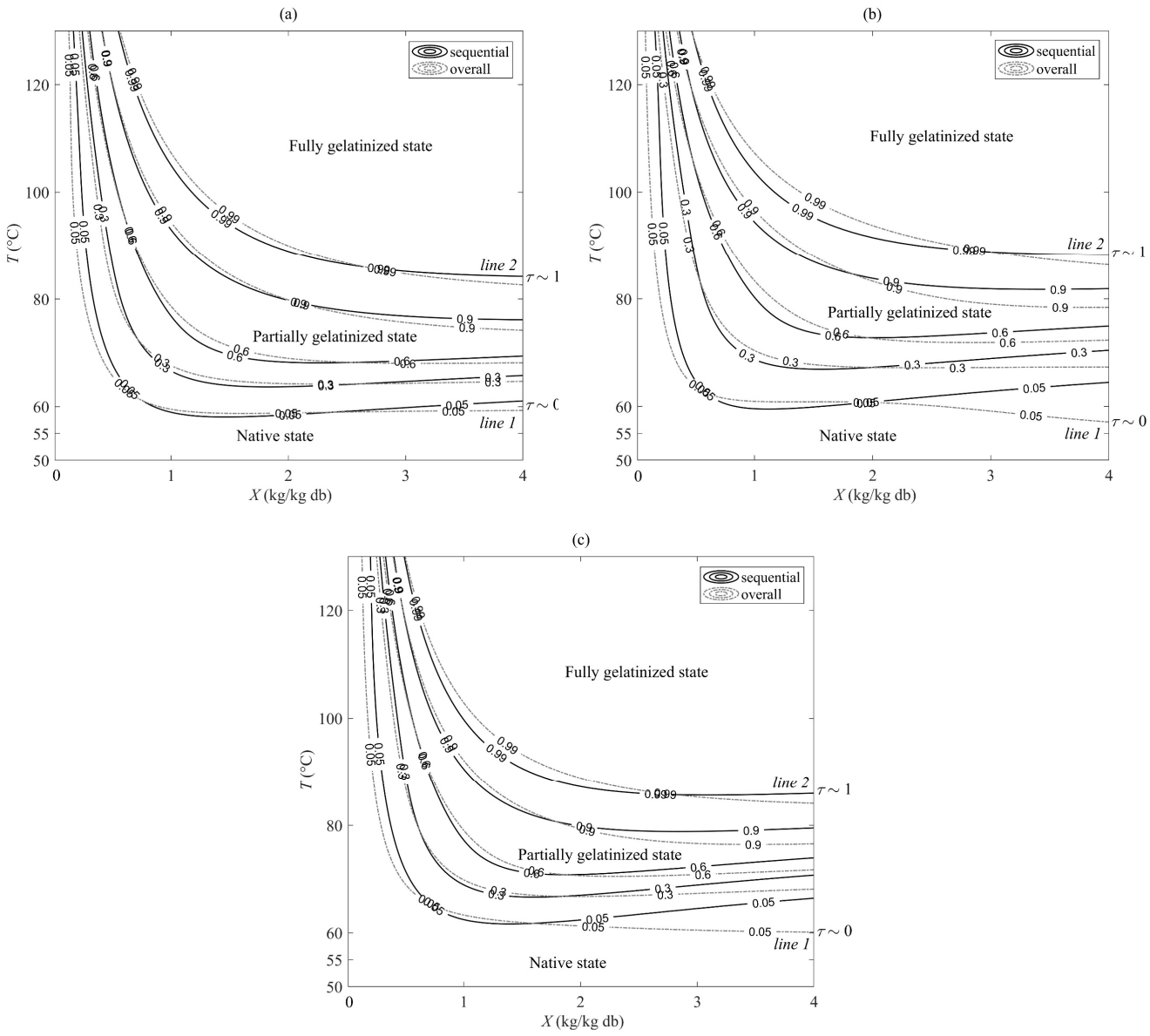

409

410 Figure 6. Modeled starch conversion diagram of lentil (a), bean (b) and chickpea (c) starch–
411 water mixture (temperature T versus water content X and isovalue lines of degree of starch
412 conversion τ) obtained with the sequential (black line) or overall (grey line) identification
413 method. Three states can be distinguished: native state (below line 1: $\tau \approx 0$), partially
414 gelatinized state (area between lines 1 and 2: $0 < \tau < 1$) and fully gelatinized state (beyond
415 line 2: $\tau \approx 1$).

416

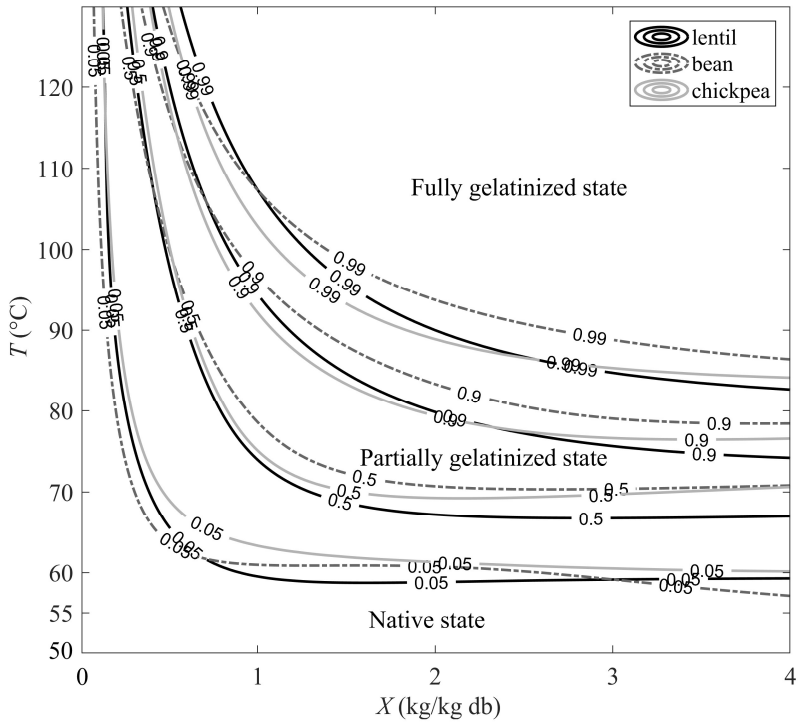

417

418 Figure 7. Comparison of modeled starch conversion diagram of the three pulses' starch–water
419 mixtures (temperature T versus water content X and isovalue lines of degree of starch
420 conversion τ) obtained with the overall identification method.

421

422 ## 4. Conclusion

423 The method of desummation and modeling of DSC heat flow thermograms presented in this
424 study improves our understanding of the starch conversion process in various T and X
425 conditions. The temperature of gelatinization can be modeled as a function of water content
426 according to the Flory-Huggins theory, as found previously for the temperature of melting.
427 The primary parameters suggest that starch undergoes melting transition regardless of water
428 content. As the water content increases, G and M endotherms overlap, producing a single
429 peak in the DSC heat flow thermogram. Both identification methods can predict the heat flow
430 of starch conversion precisely at various values for T and X. The overall identification method

generates a more precise degree of starch conversion, which can be integrated into a water transfer model to improve the cooking process for these pulses. In addition, the results suggest that the thermal behavior of lentil, bean and chickpea starches is similar despite their varietal differences. Thus, a common approach could be considered to optimize the nutritional value of all pulses.

5. Acknowledgements

We would like to thank Dr. V. Lullien and G. Maraval from INRAE (UMR IATE) for their technical help for the lentil starch extraction process. The research activities presented in this paper were supported by the Proveggas Project (22nd Unique Inter-ministerial Fund).

6. References

Blanshard, J. M. (1987). Starch granule structure and function: A physiochemical approach. In T. Gallard (Ed.), *Starch: Properties and potential* (pp. 16–54). Chicester.

Briffaz, A., Bohuon, P., Méot, J.-M., Dornier, M., & Mestres, C. (2014). Modelling of water transport and swelling associated with starch gelatinization during rice cooking. *Journal of Food Engineering*, *121*, 143–151. https://doi.org/10.1016/j.jfoodeng.2013.06.013

Briffaz, A., Mestres, C., Matencio, F., Pons, B., & Dornier, M. (2013). Modelling starch phase transitions and water uptake of rice kernels during cooking. *Journal of Cereal Science*, *58*(3), 387–392. https://doi.org/10.1016/j.jcs.2013.08.001

Carlstedt, J., Wojtasz, J., Fyhr, P., & Kocherbitov, V. (2015). Understanding starch gelatinization: The phase diagram approach. *Carbohydrate Polymers*, *129*, 62–69. https://doi.org/10.1016/j.carbpol.2015.04.045

Coffigniez, F., Briffaz, A., Mestres, C., Alter, P., Durand, N., & Bohuon, P. (2018). Multi-response modeling of reaction-diffusion to explain alpha-galactoside behavior during the soaking-cooking process in cowpea. *Food Chemistry*, *242*, 279–287. https://doi.org/10.1016/j.foodchem.2017.09.057

Coffigniez, F., Briffaz, A., Mestres, C., Ricci, J., Alter, P., Durand, N., & Bohuon, P. (2018). Kinetic study of enzymatic α-galactoside hydrolysis in cowpea seeds. *Food Research International*, *113*, 443–451. https://doi.org/10.1016/j.foodres.2018.07.030

Coffigniez, F., Rychlik, M., Sanier, C., Mestres, C., Striegel, L., Bohuon, P., & Briffaz, A. (2019). Localization and modeling of reaction and diffusion to explain folate behavior during soaking of cowpea. *Journal of Food Engineering*, *253*, 49–58. https://doi.org/10.1016/j.jfoodeng.2019.02.012

Crews, T. E., & Peoples, M. B. (2004). Legume versus fertilizer sources of nitrogen: Ecological tradeoffs and human needs. *Agriculture, Ecosystems & Environment*, *102*(3), 279–297. https://doi.org/10.1016/j.agee.2003.09.018

Cruz-Orea, A., Pitsi, G., Jamée, P., & Thoen, J. (2002). Phase Transitions in the Starch−Water System Studied by Adiabatic Scanning Calorimetry. *Journal of Agricultural and Food Chemistry*, *50*(6), 1335–1344. https://doi.org/10.1021/jf0110396

476 Donovan, J. W. (1979). Phase transitions of the starch-water system. *Biopolymers*,
477 *18*(2), 263–275. https://doi.org/10.1002/bip.1979.360180204
478 Donovan, J. W., & Mapes, C. J. (1980). Multiple Phase Transitions of Starches and
479 Nägeli Amylodextrins. *Starch - Stärke*, *32*(6), 190–193.
480 https://doi.org/10.1002/star.19800320604
481 Evans, I. D., & Haisman, D. R. (1982). The Effect of Solutes on the Gelatinization
482 Temperature Range of Potato Starch. *Starch - Stärke*, *34*(7), 224–231.
483 https://doi.org/10.1002/star.19820340704
484 Farhat, I. A., & Blanshard, J. M. (1997). On the extrapolation of the melting
485 temperature of dry starch from starch-water data using the Flory-Huggins
486 equation. *Carbohydrate Polymers*, *34*(4), 263–265.
487 https://doi.org/10.1016/S0144-8617(97)00086-6
488 Flory, P. J. (1953). *Principles of Polymer Chemistry*. Cornell University Press.
489 Gan, Y., Hamel, C., O'Donovan, J. T., Cutforth, H., Zentner, R. P., Campbell, C. A.,
490 Niu, Y., & Poppy, L. (2015). Diversifying crop rotations with pulses enhances
491 system productivity. *Scientific Reports*, *5*(1), 14625.
492 https://doi.org/10.1038/srep14625
493 Giraldo Toro, A., Gibert, O., Ricci, J., Dufour, D., Mestres, C., & Bohuon, P. (2015).
494 Digestibility prediction of cooked plantain flour as a function of water content
495 and temperature. *Carbohydrate Polymers*, *118*, 257–265.
496 https://doi.org/10.1016/j.carbpol.2014.11.016
497 Habeych, E., Guo, X., van Soest, J., van der Goot, A. J., & Boom, R. (2009). On the
498 applicability of Flory–Huggins theory to ternary starch–water–solute systems.

Carbohydrate Polymers, *77*(4), 703–712. https://doi.org/10.1016/j.carbpol.2009.02.012

Hall, C., Hillen, C., & Garden Robinson, J. (2017). Composition, Nutritional Value, and Health Benefits of Pulses. *Cereal Chemistry Journal*, *94*(1), 11–31. https://doi.org/10.1094/CCHEM-03-16-0069-FI

Holm, J., Björck, I., Drews, A., & Asp, N.-G. (1986). A Rapid Method for the Analysis of Starch. *Starch - Stärke*, *38*(7), 224–226. https://doi.org/10.1002/star.19860380704

Hoover, R., Hughes, T., Chung, H. J., & Liu, Q. (2010). Composition, molecular structure, properties, and modification of pulse starches: A review. *Food Research International*, *43*(2), 399–413. https://doi.org/10.1016/j.foodres.2009.09.001

Margier, M., Georgé, S., Hafnaoui, N., Remond, D., Nowicki, M., Du Chaffaut, L., Amiot, M.-J., & Reboul, E. (2018). Nutritional Composition and Bioactive Content of Legumes: Characterization of Pulses Frequently Consumed in France and Effect of the Cooking Method. *Nutrients*, *10*(11), 1668. https://doi.org/10.3390/nu10111668

Ratnayake, W. S., & Jackson, D. S. (2007). A new insight into the gelatinization process of native starches. *Carbohydrate Polymers*, *67*(4), 511–529. https://doi.org/10.1016/j.carbpol.2006.06.025

Tananuwong, K., & Reid, D. (2004). DSC and NMR relaxation studies of starch-water interactions during gelatinization. *Carbohydrate Polymers*, *58*(3), 345–358. https://doi.org/10.1016/j.carbpol.2004.08.003

Tosh, S. M., & Yada, S. (2010). Dietary fibres in pulse seeds and fractions: Characterization, functional attributes, and applications. *Food Research International*, *43*(2), 450–460. https://doi.org/10.1016/j.foodres.2009.09.005

Tyler, R. T., Youngs, C. G., & Sosulski, F. W. (1981). Air classification of legumes. I. Separation efficiency, yield, and composition of the starch and protein fractions. *Cereal Chemistry*, *58*, 144–148.

van der Sman, R. G. M., & Meinders, M. B. J. (2011). Prediction of the state diagram of starch water mixtures using the Flory–Huggins free volume theory. *Soft Matter*, *7*(2), 429–442. https://doi.org/10.1039/C0SM00280A